Uncertainties in the annual cycle of rainfall characteristics over West Africa in CMIP5 models

Magatte Sow [1,2]*, **Moussa Diakhaté [1]**, **Françoise Guichard [2]**, **Diarra Dieng [1,3]** and **Amadou Thierno Gaye [1]**

[1] Laboratoire de Physique de l'Atmosphère et de l'Océan - Siméon Fongang (LPAO-SF), Université Cheikh Anta Diop de Dakar, Sénégal;

[2] Centre National de Recherche Météorologique, CNRM/UMR 3589 CNRS et Météo-France/GMME/TROPICS, Toulouse;

[3] Institute of Meteorology and Climate Research (IMK-IFU), Karlsruhe Institute of Technology (KIT), Garmisch-Partenkirchen, Germany;

* Correspondence: magatte.sow@ucad.edu.sn or magatte.sow@meteo.fr; Tel.: (+221 77 314 84 68) or (+33 7 58 67 61 78)

Abstract: This study analyses uncertainties associated with the annual cycle of West African rainfall characteristics in 15 simulations of the Coupled Model Intercomparison Project phase 5 (CMIP5) over the Sahel and Guinean regions. Indices based on daily rainfall such as the frequency and the intensity of wet days, the consecutive dry days (CDD) and wet days (CWD), the 95th percentile of daily rainfall (R95) and its contribution to the cumulative monsoon rainfall (R95PTOT) have been assessed. Over both regions, TRMM, GPCP and CHIRPS observational datasets provide very consistent results on the annual cycle of precipitation but less so on the frequency of wet days. Conversely, higher uncertainties are noted on the intensity of wet days over both study areas, particularly over the Guinean region. Overall, CMIP5 simulations present much higher uncertainties in the representation of the mean precipitation climatology, often provide too early (late) onset dates over the Sahel (the Guinean region) and overestimate rainfall during the early and late monsoon phases. These errors do not compensate at the annual scale nor when considering West Africa as a whole. Results also reveal that over the Guinean region, the difficulty of models to represent the annual structure of the mean precipitation strongly involves biases in the representation of the annual cycle of the frequency of wet days. We found strong uncertainties in the simulation of the CWD and the CDD over both areas. Conversely for R95p and R95PTOT, the uncertainties in CMIP5 models appear somewhat weaker, but the magnitude of R95 is largely underestimated in most models.

Keywords: West Africa, rainfall, annual cycle, CMIP5 models, onset, cessation, extremes, uncertainties

---

1. Introduction

The annual cycle of monsoon precipitation is a primary feature of the West African Climate (e.g. [1–3]). In this region, rainfall mainly falls from April to October, with major differences between the wetter Guinean region where precipitation displays two annual peaks (in June and in September) and the more arid Sahelian region, where it displays a single peak centred on August. In this tropical area, observations also underline the strength of mesoscale convective events [4] which accounts for a large amount of annual cumulative rainfall [5,6]. At the same time, dry spells events are also relatively frequent in West Africa during the monsoon [7,8] and were particularly severe during the drought decades of the 70's and 80's [9]. More broadly, in the last decades, an alteration of periods with extreme rainfall events and dry conditions has led to a succession of flood/drought years [10,11]. Changes in the annual cycle of monsoon precipitation have also been identified, with notably a trend toward more rainfall during the second part of the monsoon in the last 30 years [12–15]. These important traits of precipitation have strong implications for social and economic sectors which are strongly linked to

agricultural and water resources in West Africa [16]. Furthermore, given the high vulnerability of this region, any climatic changes in monsoon precipitation (either its amount, annual cycle, intensity and intraseasonal distribution) is likely to affect many socio-economic developments [17–21]. According to the Intergovernmental Panel on Climate Change report [22], a number of studies indicate that climate change induced by increasing anthropogenic greenhouse gas (GHG) concentrations is expected to delay the onset of Sahelian precipitation [23], to intensify the hydrological cycle and to increase the occurrence of extreme precipitation events [10,24–29]. This implies that West African countries will be indeed affected by global warming in many areas and will face important adaptation challenges.

However, studies based on Coupled Model Intercomparison Project (CMIP) phase 3 and 5 show that the representation of the West African Monsoon (WAM) mean state as well as its response to global warming are both highly model-dependent in many ways [30]. As a consequence, model-based projections of the WAM and of the Sahel climate are highly uncertain [31]. It is therefore important and valuable to more precisely characterize these uncertainties in climate models over West Africa. The CMIP5 multi-model ensemble consists in more than 40 climate models, with generally several realizations (or members) performed under four different Representative Concentration Pathways (RCPs). It seems to be virtually impossible for most groups working on dynamical downscaling and/or impacts with limitations in computing resources and/or data storage capacity to deal with such of large ensemble. However, scientists have to deals with these uncertainties when synthesizing climate information for impacts studies. Therefore, there is a need to better characterize these uncertainties, in particular their spatial and temporal characteristics. This study focusses on the annual cycle of precipitation over West Africa, and its main goal is to analyse and evaluate the uncertainties associated with its simulation by CMIP5 models, including its mean characteristics, as well as the annual cycle of wet and dry spells from the Gulf of Guinea to the Sahel. The paper is organized as follow: in section 2 we present the CMIP5 models, the satellite data used for model evaluation as well as the methodology. Results and discussions are presented in section 3 and finally, conclusions are given in section 4.

2. Data and Methods

In this study, daily precipitation corresponds to the variable from which all our analyses are carried out. We retrieved it for 15 CMIP5 historical simulations provided by 11 institutions (Table 1) as well as three different satellite-based estimates. We chose to use three observationally-based estimates in order to partially account for uncertainties in existing observations datasets [32]. These are (i) the Climate Hazards Group Infrared Precipitation with Station data (CHIRPS), which is a blend of Climate Hazards Group Precipitation climatology, satellite infrared measurements and direct rain gauge measurements (which are sparse over West Africa) and is available from 1981 to present at a 0.5° x 0.5° resolution [33], (ii) the Global Precipitation Climatology Project 1 Degree Daily (GPCP 1DD), available from 1996 to present with a 1° x 1° resolution [34] and (iii) the Tropical Rainfall Measuring Mission (TRMM) Multi-satellite Precipitation Analysis (TMPA) 3B42v7 research derived daily product , available from 1998 to present at a 0.25° x 0.25° resolution [35].

The CMIP5 daily outputs have been compared to these observationally-based daily rainfall datasets. The different simulations as well as the three satellite estimates are all provided on different grids, whose width varies from less than 1° to more than 3° (see Table 1). Therefore, for the comparison presented below, all the datasets were regridded to a spatial resolution of 0.5° × 0.5° using the bilinear interpolation technique.

Due to the datasets availability (CHIRPS starts from 1981 and most of CMIP5 historical simulations end in 2004), analyses are focused over period from 1985 to 2004. The Sahel and the Guinean regions (boxes on Figure 1) are analysed separately and annual cycles of spatial averaged total daily rainfall and their characteristics over these two regions have been computed. As recalled in the introduction, this separation is motivated by the fact that these two climate regions display quite distinct rainfall regimes [36–38]. The Sahel region is characterized by one rainy season occurring during the period from June to September, while, the rainfall regime over the Gulf of Guinea presents a bimodal structure

with one peak in Jun during northward migration of the Inter-Tropical Convergence Zone (ITCZ) and another one in September during the southward return of the ITCZ.

For the rainfall characteristic, different indices, as defined by the Expert Team on Climate Change Detection and Indices (ETCCDI [39]), are considered here in order to quantify daily precipitation characteristics:

- The frequency of daily precipitation events is the number of events with precipitation greater than 1 mm;
- The Simple daily intensity index is the mean intensity of daily precipitation events;
- The Consecutive Dry Days (CDD) period is the number of consecutive dry sequences of more than 5 days (dry spells). A dry day is defined as a day with precipitation less than 1 mm;
- The Consecutive Wet Days (CWD) period is the number of consecutive wet sequences lasting more than 5 days (wet spells). A wet day is defined as a day with precipitation greater than 1 mm;
- The 95th percentile of daily precipitation events (R95) is the value above which 5% of the daily precipitation events are found;
- Total precipitation with respect to the R95p (R95ptot) is the fraction of precipitation accounted for by the very wet days (daily rainfall above the R95).

Percentile-based threshold indices (e.g. R95 and R95ptot) are used to characterize high-intensity precipitation events because the number of exceedances is more evenly distributed in space and they are meaningful in all regions, thus allowing for spatial comparisons over large areas [39]. The reference percentile (95th percentile) used for the count of exceedances is based on historical values, and a day is considered to be wet if precipitation amount exceeds 1 mm.

Finally, in order to characterize the timing of the monsoon season and its length, we use the method of Liebmann [3] to determine the onset and cessation dates of the wet season over the Sahel and the Guinean region. The method can be summarized as follows: Firstly the long-term annual-mean daily average and the long-term daily average for each day of the year is computed. Starting from 1 January, the sum of the difference between the climatological daily average and the climatological annual-mean daily average gives the climatological accumulated anomaly. The day after which the value of the accumulated anomaly reaches its absolute minimum is the onset date since, from that day onward for this particular year, accumulated precipitation exceeds what would be expected from climatology. Conversely, the day on which accumulated anomaly reaches the maximum is the cessation date of the wet season.

Table 1. Basic information for the 15 CMIP5 models used in this study.

Modelling Center	Institution	Model Name	Resolution
Beijing Climate Center, China Meteorological Administration	BCC	BCC-CSM1.1(m)	2.79°x2.81°
Canadian Centre for Climate Modelling and Analysis	CCCma	CanESM2	2.79°x2.81°
Centre National de Recherches Météorologiques/Centre Europeen de Recherche et Formation Avancees en Calcul Scientifique	CNRM-CERFACS	CNRM-CM5	1.40°x1.40°
National Center for Atmospheric Research	NCAR	CCSM4	0.94°x1.25°
Commonwealth Scientific and Industrial Research Organization in collaboration with Queensland Climate Change Centre of Excellence	CSIRO-QCCCE	CSIRO-Mk3.6.0	1.86°x1.87°
EC-EARTH consortium	EC-EARTH	EC-EARTH	1.12°x1.12°
Met Office Hadley Centre(additional HadGEM2-ES realizations contributed by Instituto Nacional de Pesquisas Espaciais)	MOHC	HadGEM2-ES	1.25°x1.85°
Institut Pierre-Simon Laplace	IPSL	IPSL-CM5A-LR	1.89°x3.75°
Institut Pierre-Simon Laplace	IPSL	IPSL-CM5A-MR	1.27°x2.50°
Japan Agency for Marine-Earth Science and Technology, Atmosphere and Ocean Research Institute(The University of Tokyo), and National Institute for Environmental Studies	MIROC	MIROC-ESM	2.79°x2.81°
Atmosphere and Ocean Research Institute (The University of Tokyo), National Institute for Environmental Studies, and Japan Agency for Marine-Earth Science and Technology	MIROC	MIROC4h	0.56°x1.41°
Atmosphere and Ocean Research Institute (The University of Tokyo), National Institute for Environmental Studies, and Japan Agency for Marine-Earth Science and Technology	MIROC	MIROC5	1.40°x1.41°
Max-Planck-Institut für Meteorologie (Max Planck Institute for Meteorology)	MPI-M	MPI-ESM-LR	1.86°x1.87°
Max-Planck-Institut für Meteorologie (Max Planck Institute for Meteorology)	MPI-M	MPI-ESM-MR	1.86°x1.87°
Meteorological Research Institute	MRI	MRI-CGCM3	1.12°x1.12°
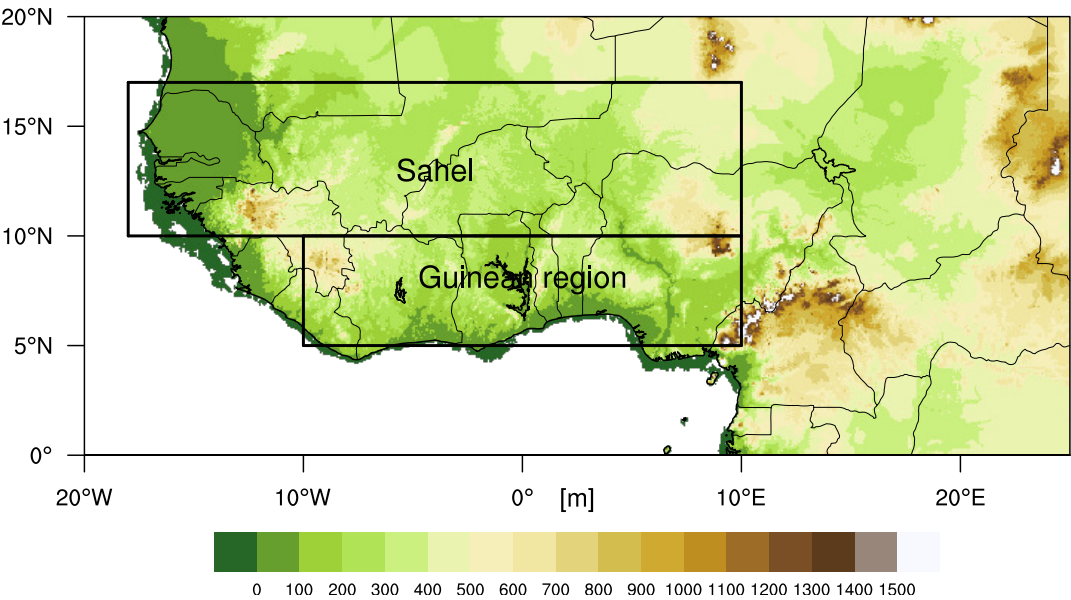
Figure 1. Topography (in meters) of the study area (West Africa). The black boxes highlight the two-considered subregions (Sahel and Guinean region).

3. Results

3.1. The annual cycle of mean precipitation, intensity and frequency of wet days

This section focuses on the annual cycle of precipitation, as well as those of precipitation intensity and frequency of wet days. It provides an inter-comparison of CMIP5 results with observational datasets (CHIRPS, TRMM and GPCP). We start with the analyse of the annual cycle of monthly-mean precipitation. Figure 2a indicates that CHIRPS, TRMM and GPCP provide a very close depiction of this cycle over the Sahel (see also Figure S1), while models capture reasonably well the broad temporal structure of the annual cycle with a peak in August though with a very large spread of the amplitude from less than 2 to more than 8 mm/day in August). Likewise, over the Guinean region, the observational datasets agree quite well even though the "litle dry saison" [40] is more marked in TRMM and GPCP than in CHIRPS. By contrast, the annual cycles in CMIP5 models display a variety of shapes and only CNRM-CM5, MIROC5 and MIROC4h capture the bimodal structure of this cycle (Figure 2b).

During the core of the monsoon (July-August), over the Sahel, only two models, CSIRO-Mk3 and MIROC5 present a substantial positive biases compared to satellite datasets (about 2 mm/day), while most of the other models underestimate the magnitude of rainfall with peaks as low as 2 mm/day. In August, MPI-ESM-MR, MPI-ESM-LR, EC-EARTH, MIROC4h, CCSM4GHG and CNRM-CM5 perform relatively well compared to observations with peaks between 6 and 7 mm/day. This could perhaps be related to a better representation of the African Easterly Waves (AEWs) in these models during this month [41,42], although several other causes are possible. The ensemble mean (ENSEMBLE) performs better than several models but still underestimates the core monsoon rainfall.

For the Guinean region, as for the Sahel, a large spread among models is also present, but in contrast with the Sahel, most models overestimate the magnitude of precipitation during the monsoon and the ENSEMBLE fails to reproduce the bimodal character of precipitation. In fact, only 3 models (CNRM-CM5, MIROC5 and MRI-CGCM3) are able to reproduce well either the June or the September peak. For instance, the CNRM-CM5 first peak (around 9 mm/day) occurs in June as observed, while the second one (around 10 mm/day) is observed in August instead of September. MRI-CGCM3 similarly displays its peaks in June (6 mm/day) and August (5.5 mm/day). The second peak in MIROC5 (12.5 mm/day) is observed at the right time but the first one (12 mm/day) occurs one month too late, in July.

In general, models who underestimate/overestimate precipitation during the core monsoon months do so throughout the monsoon season but almost all models also simulate precipitation outside of the monsoon period, e.g. in March in the Sahel when there is hardly any rain observed.

Focussing now on the annual cycle of the frequency of wet days, satellite datasets are found to agree reasonably well, and more so over the Sahel. There, the maximum frequency occurs during the core monsoon season in August, and it is lower in TRMM and GPCP than in CHIRPS (by 10-20%). A higher frequency is observed in CHIRPS over the Guinean region too, but there, satellite datasets display a larger spread in Spring (April-May), reaching about 30%. Interestingly, the annual cycle of the frequency of wet days displays a well-defined double peak structure in GPCP and CHIRPS, while this characteristic is much less pronounced in TRMM. CMIP5 simulations capture very approximately the structure of these annual cycles (Figure 2c,d), with most often strong positive biases, i.e. it rains more frequently in simulations over both regions. In August over the Sahel, CSIRO-Mk3, EC-EARTH and IPSL-CM5A-LR display the largest biases, of respectively +10, +8 and +8 days compared to observed and biases can reach more than 50% during the monsoon. Over the Guinean region, the bimodal structure associated with the frequency of wet days is lacking in CMIP5 models, most of them simulate a relatively constant or slightly increasing frequency from May to October. Indeed, it is raining almost every day in several models, with biases then reaching about 100%. Finally, over both regions, models largely overestimate the frequency of wet days prior to and following the monsoon season (up to 200% in May over the Sahel). This overestimation may be related to well known issues with the

representation of the diurnal cycle of convective precipitation in models (e.g. [43,44]) when convective inhibition is not preventing the onset of convection. The magnitude of the frequency of wet days is expected to be sensitive to the grid size. However, we did not find any clear evidence of this sensitivity when comparing models from this perspective. Conversely, in observational datasets, the frequency of wet days increases when considering a coarser $1°x1°$ grid , although the difference remains relatively small (See Figure S3).

Shifting now to the annual cycle of the intensity of wet days, TRMM and GPCP are again very close to each other over the Sahel, with values somewhat higher than in CHIRPS (by about 20% in August). The situation is different over the Guinean region, where satellite datasets display the wider spread; large uncertainties are noted in observational datasets especially from January to May (with a difference reaching 100% between CHIRPS and TRMM in April). Furthermore, they display very distinct structures of the annual cycle of wet days intensity. CHIRPS indicate a well defined maximum in July, which is higher than in TRMM and GPCP; while in these two datasets, the intensity does not fluctuate much from June to September.

Models generally simulate a peak of intensity in August over the Sahel (Figure 2e), but with strong uncertainties in the amplitude. MIROC4h is the only model displaying a higher intensity that satellite datasets. BCC-CSM1, IPSL-CM5A-LR, IPSL-CM5A-MR and MRI-CGCM3 show a significant underestimation between 2 and 4 mm/day (i.e. an underestimation typically comprised between 200 and 500%).

Over the Guinea region, there is also a wide spread among models on the representation of the intensity of wet days, but with a dominantly negative bias on the amplitude of the signal in most models (Figure 2f). In term of temporal evolution, several models display a unimodal structure of the intensity of wet days, but given the uncertainties in observational datasets, it is not possible to conclude as to which models perform better.

Finally, it is noticeable that over both regions and in observational datasets as well as in models, the annual cycles of the intensity and of the frequency of wet days are both very strongly correlated with the annual cycle of the mean precipitation (see Supplementary Table S1), which implies in particular that model biases in their annual cycles are linked.

In summary, one can retain that the annual cycle of wet days intensity is in general poorly represented in models over the two areas, with particularly large uncertainties regarding the magnitude of the intensity of wet days. However, in contrast with the Sahel, in the Guinean region, models uncertainties in the annual cycle of precipitation are not dominated by uncertainties in the frequencies of wet days. In particular, biases in the representation of the bimodal structure over the Guinean region appears to be more closely related to the representation of the intensity than the frequency of wet days in models.
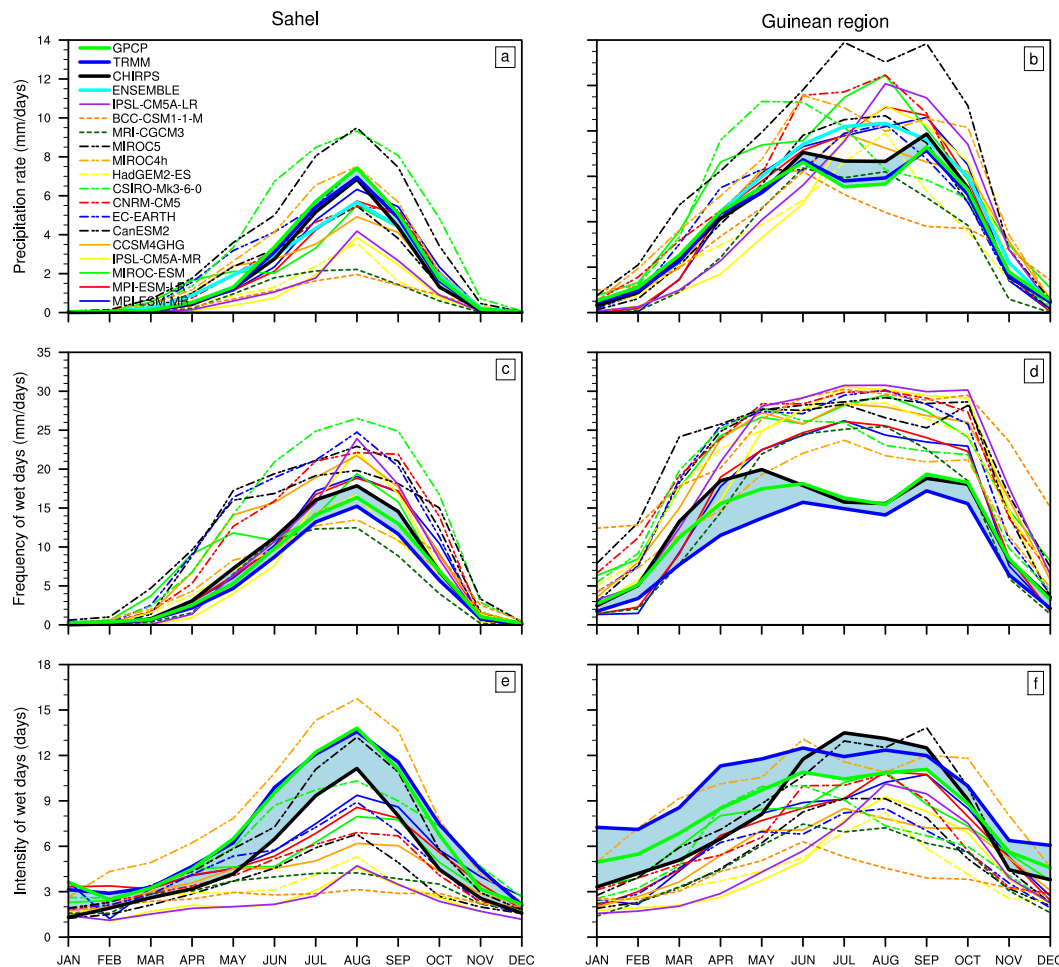
Figure 2. Annual cycle of rainfall (**a**,**b**), frequency (**c**,**d**) and intensity of wet days (**e**,**f**) over the Sahel (left) and Guinean region (right) from CHIRPS (black), TRMM (blue), GPCP (green) and 15 CMIP5 models and their ensemble mean (cyan). The shaded area indicate the spread between the three satellite estimates.

Quantitative diagnostics within Taylor diagrams confirm these findings (Figure 3, where CHIRPS is retained as a the dataset to which other satellites and model datasets are compared). For the annual cycle of precipitation and frequency of wet days over the Sahel, TRMM and GPCP are very strongly correlated (>0.99) with CHIRPS and have a normalized standard deviation close to 1 (slightly > 1 for the precipitation and slightly < 1 for the frequency), consistently with the fact that TRMM and GPCP indicate a lower frequency of wet days over that area. For the annual cycle of the intensity of wet days, despite the strong correlation (between 0.95 and 0.99), TRMM and GPCP have a normalized standard deviation of 1.25, again consistent with their higher values noted in Figure 2e.

In line with results presented in Figure 2b,d,f, over the Guinean region, the correlation of TRMM and GPCP with CHIRPS is stronger on the annual cycle of the mean precipitation than on the frequency and intensity of wet days. The normalized standard deviation is slightly less than 1 on the annual cycle of precipitation and frequency of wet days, as TRMM and GPCP indicate a lower frequency of wet days than CHIRPS (Figure 2d).

In models, the annual cycles of the mean precipitation, of the frequency and intensity of wet days correlate well with CHIRPS over the Sahel, confirming the fact that in this area, models are in general able to qualitatively capture the unimodal structure of the annual evolution of precipitation

(Figure 3a). However, the distribution of values is scattered along the standard deviation axis, which indicate how the uncertainties in the amplitude of precipitation are important in CMIP5 models over the Sahel. For some models (MPI-ESM-MR, MIROC-ESM, CNRM-CM5, MPI-ESM-LR, EC-EARTH, MIROC4h, CanESM2), and for the ENSEMBLE, the normalized standard deviation is close to 1 but some others models display very strong (1.55 for CSIRO-Mk3 and 1.44 for MIROC5) or weak (0.30, 0.37, 0.46 respectively for BCC-CSM1, MRI-CGCM3, HadGEM2) values. Figure 3a also reveals that over the Sahel, uncertainties in total precipitation come from both uncertainties in the intensity and on the frequency of wet days. Over the Guinean region, Figure 3b shows much weaker correlations compared to the Sahel. This is partly due to the poor representation of the bimodal structure of precipitation in the CMIP5 models over this region. Regarding the normalized standard deviations values, the distribution appears less scattered compared to the Sahel region in agreement with previous conclusions from Figure 3a,b. In contrast with the Sahel region, Figure 3b also indicates that over the Guinean region, the uncertainties in daily total precipitation dominantly involve those in the frequency of wet days.Most of the models fail to reproduce the frequency of wet days, which also contributes to the poor representation of the bimodal structure of precipitation in this area.

In summary, over both the Sahel and Guinean regions, TRMM, GPCP and CHIRPS datasets provide very consistent results on the annual cycle of precipitation but less so on the frequency of wet days. Conversely , uncertainties are noted on the intensity of wet days over both areas, but especially over the Guinean region. On the other hand, CMIP5 models present very high uncertainties in the seasonal cycle of precipitation. Separate analysis of the frequency and intensity of the wet days reveal that over the Sahel, the uncertainties are important on both the amplitude of frequency and intensity of wet days. It also reveals that over the Guinean region, the difficulty of models to represent the annual structure of the mean precipitation is dominated by biases in the representation of the annual cycle of the frequency of wet days. Finally, it is difficult to conclude regarding the simulation of the temporal structure of the annual cycle of the intensity of wet days over the Guinean region, because of uncertainties in observational datasets.
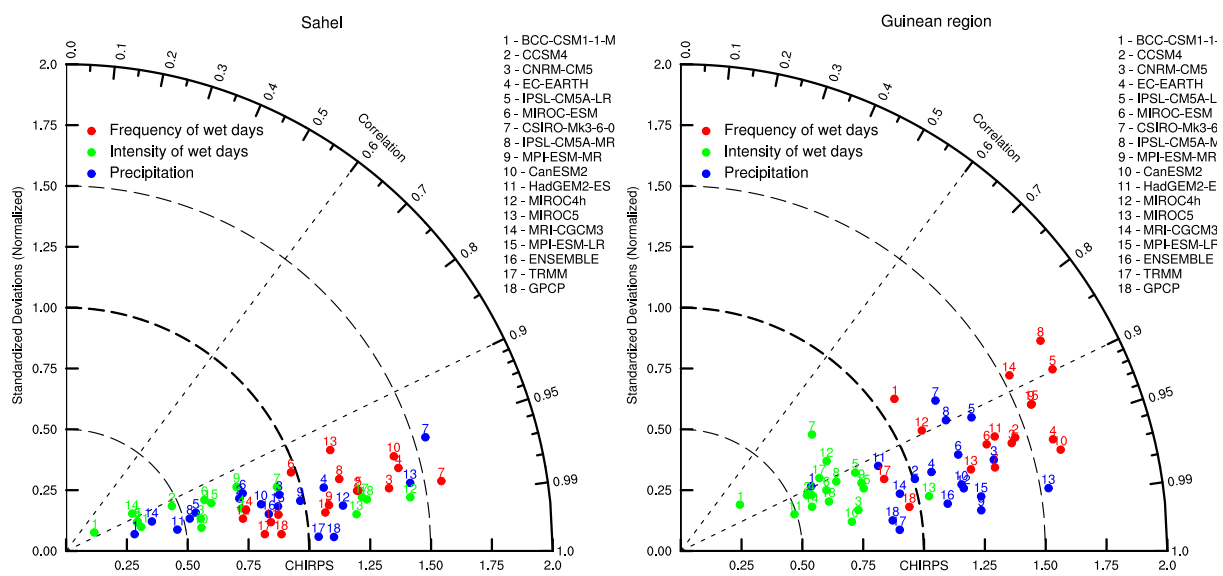
Figure 3. Taylor diagrams of the annual cycle of daily mean rainfall (mm/day), intensity and frequency of wet days from 1985 to 2004 over the Sahel (left) and the Guinean region (right) for TRMM, GPCP and 15 CMIP5 models compared to CHIRPS.

3.2. Resulting precipitation amounts at the annual time scale over the Sahel and Guinean regions

Over West Africa, errors in the simulation of the latitudinal position of the ITCZ can be a primary source of precipitation biases (e.g. [45]), and can be associated with compensating errors between the Sahel and Guinean regions. For instance, if the ITCZ is located too much to the South, it can lead to an underestimation of precipitation amounts over the Sahel and potentially to an overestimation over the Guinean zone. Table 2 allows to assess this issue by comparing the annual mean precipitation and the biases (differences are computed with respect to CHIRPS) over both regions and over "West Africa" (defined here as the ensemble of the two regions).

In agreement with previous results, the differences between the observational datasets are weak. TRMM and GPCP indicate slightly more precipitation over the Sahel (+49 mm and +97 mm respectively) and slightly less over the Guinean region (-86 mm and -89 mm respectively), leading to slightly more precipitation over West Africa (+65mm and +21 mm respectively). The differences remain below 10% except between CHIRPS and GPCP over the Sahel (+14%), but they indicate compensations between the Sahel and the Guinean region which narrow the range of differences when considering West Africa as a whole. Table 2 also indicates that it rains about twice more in the Guinean region compared to the Sahel. Differences are more important in CMIP5 models, and vary from -12 mm (MPI-ESM-LR) to +689 mm (CSIRO-Mk3) over the Sahel. In general, models who underestimate/overestimate precipitation during the core monsoon months do so throughout the monsoon season but almost all models also simulate precipitation outside of the monsoon period, e.g. in March in the Sahel when there is hardly any rain observed. Despite this additional unrealistic source of precipitation, on an annual-mean basis, we found that there are more models displaying a negative bias over the Sahel (which represents -20 to -65% of CHIRPS annual rainfall). Conversely over the Guinean region, model biases are dominantly positive and represent 1 to 64% (+20 mm to +955 mm) of CHIRPS annual rainfall excepted for MRI-CGCM3 (-419 mm), HadGEM2-ES (-293 mm), BCC-CSM1-1-M (-262 mm) and IPSL-CM5A-MR (-18 mm). However, on a model-by-model basis, we do not found many cases of underestimation over the Sahel combined with an overestimation over the Guinean region (see also Figure S2). Rather, in 66% of the models, it rains either too much or not enough over both regions, which points to a primary bias in the simulation of the West African rainfall (rather than biases in its latitudinal distribution), where about half of the models overestimates precipitation and the other half underestimates it.

Table 2. Annual cumulative precipitation (mm) and precipitation difference (in mm and percentage) between CHIRPS and GPCP, TRMM, CMIP5 model's simulations and their ensemble mean over the Sahel, Guinean region and West Africa averaged over the period 1985-2004 for CHIRPS and models and over the period 2000-2010 for GPCP and TRMM.

	Sahel		Guinean region		West Africa	
CHIRPS	**686**		**1492**		**852**	
GPCP	+97	(+14 %)	-59	(-4 %)	+65	(+8 %)
TRMM	+49	(+7 %)	-86	(-6 %)	+21	(+2 %)
BCC-CSM1-1-M	-443	(-65 %)	-262	(-18 %)	-406	(-48 %)
CanESM2	-144	(-21 %)	+20	(+1 %)	-110	(-13 %)
CCSM4	-114	(-17 %)	+86	(+6 %)	-73	(-9 %)
CNRM-CM5	+71	(+10 %)	+377	(+25 %)	+134	(+16 %)
CSIRO-Mk3-6-0	+689	(+100 %)	+260	(+17 %)	+600	(+70 %)
EC-EARTH	+221	(+32 %)	+90	(+6 %)	+194	(+23 %)
HadGEM2-ES	-315	(-46 %)	-293	(-20 %)	-310	(-36 %)
IPSL-CM5A-LR	-323	(-47 %)	+56	(+4 %)	-245	(-29 %)
IPSL-CM5A-MR	-345	(-50 %)	-18	(-1 %)	-277	(-33 %)
MIROC-ESM	-165	(-24 %)	+196	(+13 %)	-90	(-11 %)
MIROC4h	+238	(+35 %)	+487	(+33 %)	+289	(+34 %)
MIROC5	+609	(+89 %)	+955	(+64 %)	+680	(+80 %)
MPI-ESM-LR	-12	(-2 %)	+61	(+4 %)	+3	(0 %)
MPI-ESM-MR	+57	(+8 %)	+48	(+3 %)	+55	(+6 %)
MRI-CGCM3	-409	(-60 %)	-419	(-28 %)	-411	(-48 %)
ensmean	-7	(-1 %)	+119	(+8 %)	+19	(+2 %)

3.3. Timing and length of the monsoon season

As emphasized above, the models do not provide a proper depiction of the annual cycle of precipitation and it is important to characterize these differences in more details. To do so, here we determine the length of the wet season, as well as its start and end dates.

Figure 4 shows the daily accumulated precipitation anomalies, the onset, the cessation and half of the cumulative precipitation dates from observations and CMIP5 simulations over the Sahel and the Guinean region. The evaluation is performed with CHIRPS and CMIP5 models for the period 1985-2005, and over 2000-2010 for TRMM and GPCP reference data sets. Results shows that the Mean onset date is similar in the different observation products for the Sahel region ($1st$ of June), while the cessation date (first two weeks of October) is earlier in CHIRPS and later in GPCP with a difference of less than 10 days. In CMIP5 models, except for MPI and IPSL simulations, the onset occur earlier than in observational datasets, by up to several weeks (from 21 April for MIROC-ESM to 22 May for HadGEM-ES) while cessation dates are closer to observed, even though sometimes a bit later (6 October for MIROC4h to 24 October for BCC-CSM1). Conversely in MPI and IPSL models, the monsoon onset occurs later (from 8 to 17 Jun) and the cessation is also later in the year, up to 22 October.

Rainfall is not distributed uniformly during the monsoon: it rains more during the second half of the monsoon according to CHIRPS and TRMM. This characteristic is at least partly captured by most models (Figure 4b). Over the Guinean region, onset dates from observational datasets are observed around 13 April and cessation dates around 31 October. These dates correspond to the start of the first season and the end of the second season, which are both separated by the little dry season. In our case this dry phase is not very pronounced that's why we can use this method (keeping in mind that it can't provide the intermediate onset and cessation dates over this region). Half of the annual cumulative rainfall is recorded around 20 July, which is close to to middle of the monsoon season and indicates that there is about as much rainfall during the first and second half of the monsoon season.

In CMIP5 models, except for MIROC-ESM, onset dates occur later, from the 1st to 24 May and cessation dates sometimes earlier (around mid-October) than the observed dates. In most models, half of the annual cumulative rainfall is recorded during the first half of the wet season, a date which varies

from 20 June (CSIRO-Mk3) to 10 August (IPSL-CM5A-MR). Finally, there is a slight length asymmetry between the second (shorter) and third (longer) quartile in most models, in qualitative agrement with observations.

In summary, observational datasets show a good agreement in their determination of the onset and cessation dates of the rainy season over the two regions. These results are consistent with Dunning [2] who found good correlations (around 0.88 to 0.91) of the onset and cessation dates provided by satellite datasets over Africa using this method. CMIP5 models often provide too early onset and/or too late cessation dates over the two subregions meaning that most of models overestimate the precipitation during the early and late monsoon, a result which is also consistent with Seth [46]. However, we do not find any obvious link between model errors in the timing or length of the monsoon season and annual precipitation (see Table S1)
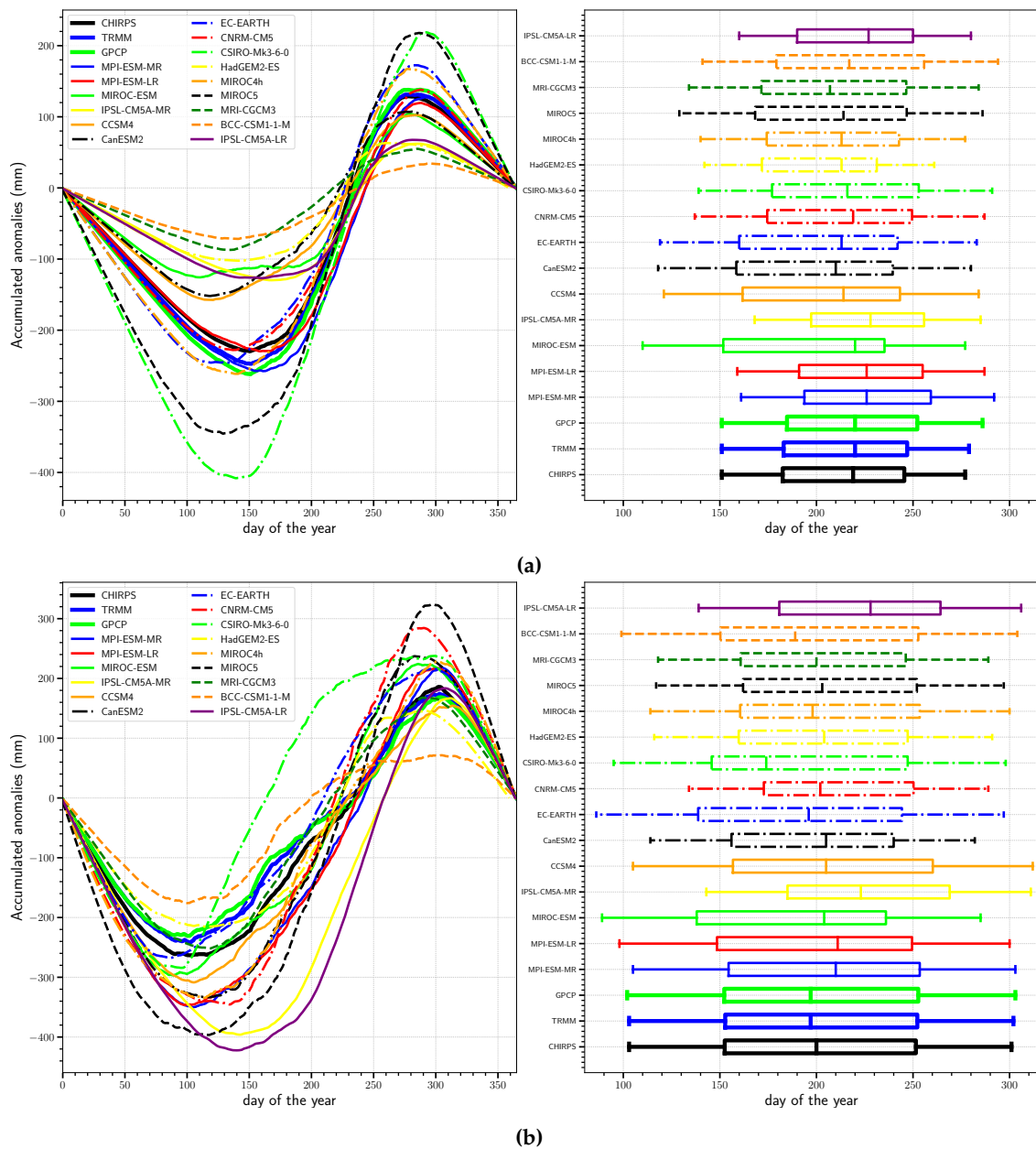
Figure 4. Daily accumulated-anomalies of precipitation (left); onset, cessation and half of the cumulative precipitation dates (right) from observations (full lines) and CMIP5 models simulations (dashed, dotted and dash-dotted lines) over the Sahel (a) and the Guinean region (b); averaged over 1985-2004 for CHIRPS and models and over 2000-2010 for TRMM and GPCP. The first and third quartile, as well as the median are indicated.

3.4. The annual cycle of extreme precipitation indices

In this section, we focus on the annual cycle of extreme precipitation indices (presented in section 2) provided by satellite datasets and CMIP5 models (Figure 5).

First, Figure 5a shows that over the Sahel, the structure of the annual cycle of 5-days CWD is very similar in the three satellite datasets, but TRMM and GPCP provide much less wet spells than CHIRPS. Over the Guinean region, more important differences are noted in observational datasets (Figure 5b) with again less CWD in TRMM and GPCP, and an almost unimodal structure in TRMM (with a maximum in September), contrasting with CHIRPS, which displays a well defined first maximum in May. Over the Sahel, some of the models (MIROC-ESM, MPI-ESM-MR, MPI-ESM-LR,

IPSL-CM5A-MR, IPSL-CM5A-LR, MIROC5, HadGEM2, EC-EARTH, CCSM4GHG and CSIRO-Mk3 simulate a CWD peak in August as observed, but uncertainties in the amplitude are very high in most models (CSIRO-Mk3, CCSM4GHG, EC-EARTH, IPSL-CM5A-LR, IPSL-CM5A-MR). Several models fail to represent the observed unimodal structure. For instance, in MRI-CGCM3, the amplitude of the peak is well captured, but it occurs too early, in July, while in EC-EARTH, CanESM2, CNRM-CM5, CCSM4GHG and MIROC5, the annual cycle of CWD present a multi-peak structure. A few models performs quit well for CDD in the Sahel (Figure 5c). However, it is important to note that, the MRI-CGCM3 model, which performs the best on wet spells also performs the worst on dry spells. Similarly, the IPSL provides a reasonable simulation of CDD, but it also largely underestimate the mean precipitation.

Over the Guinea region, very high uncertainties are also noted in models (Figure 5b). Most of the models represent two peaks for CWD and, even more than in the Sahel, they all largely overestimate the magnitude of the CWD (by more than 100%). In addition, over the Guinean region, models are unable to capture the peak of CDD observed from July to August (Figure 5d). Finally, the model biases noted on CDD are relatively lower than those obtained on CWD over both regions, and appear to be relatively less important over the Guinea region than over the Sahel. Therefore, beyond uncertainties in observational datasets, CWD appear to be too much numerous in almost all models over the two regions. Mirroring differences in CWD, CDD are more numerous in TRMM and GPCP than in CHIRPS while their annual structure are relativity close. In particular, the three datasets indicate an increase of CDD during the little dry season over the Guinean region (Figure 5d), which is not seen by CMIP5 models. In addition, over the Guinean region, models are unable to capture the peak of CDD observed from July to August (Figure 5d). Finally, the model biases noted on CDD are relatively lower than those obtained on CWD over both regions, and appear to be relatively weaker over the Guinea region than over the Sahel.

For the 95th percentile of daily precipitation, uncertainties are overall stronger than for the previous indices in observational datasets as well as in CMIP5 models. It takes values around 20 mm/day for CHIRPS and 30 mm/day (34 mm/day) for GPCP (TRMM) in August over the Sahel. Over the Guinean region, as noted for the intensity (Figure 2b), differences between datasets are larger prior to the little dry season. Despite these large differences among datasets, it appears that over both regions, most models underestimate the 95th percentile, i.e. they simulate more wet days and CWD, but the intensity and extrema of precipitation are much less than observed.

Finally, the annual cycle of the fraction of precipitation accounted by the very wet days is shown in Figure 5g,h. Its structure, with a minimum during the monsoon season (around 20%), is relatively well captured by the models compared to the previous indices (this is not unexpected as this index does not involve model biases in the simulation of precipitation). The main differences are underestimations of this index in April-May over the Sahel, and during the little dry season in the Guinean region. Overall, this fraction is relatively small, which suggests that model errors in the highest precipitation values cannot explain a large part of the errors in the mean precipitation. Note that, as for the frequency and intensity of wet days, our comparison and conclusions are not much sensitive to the grid size over which extreme indices are computed for satellite data, at least in this range of resolution (see Figure S4).
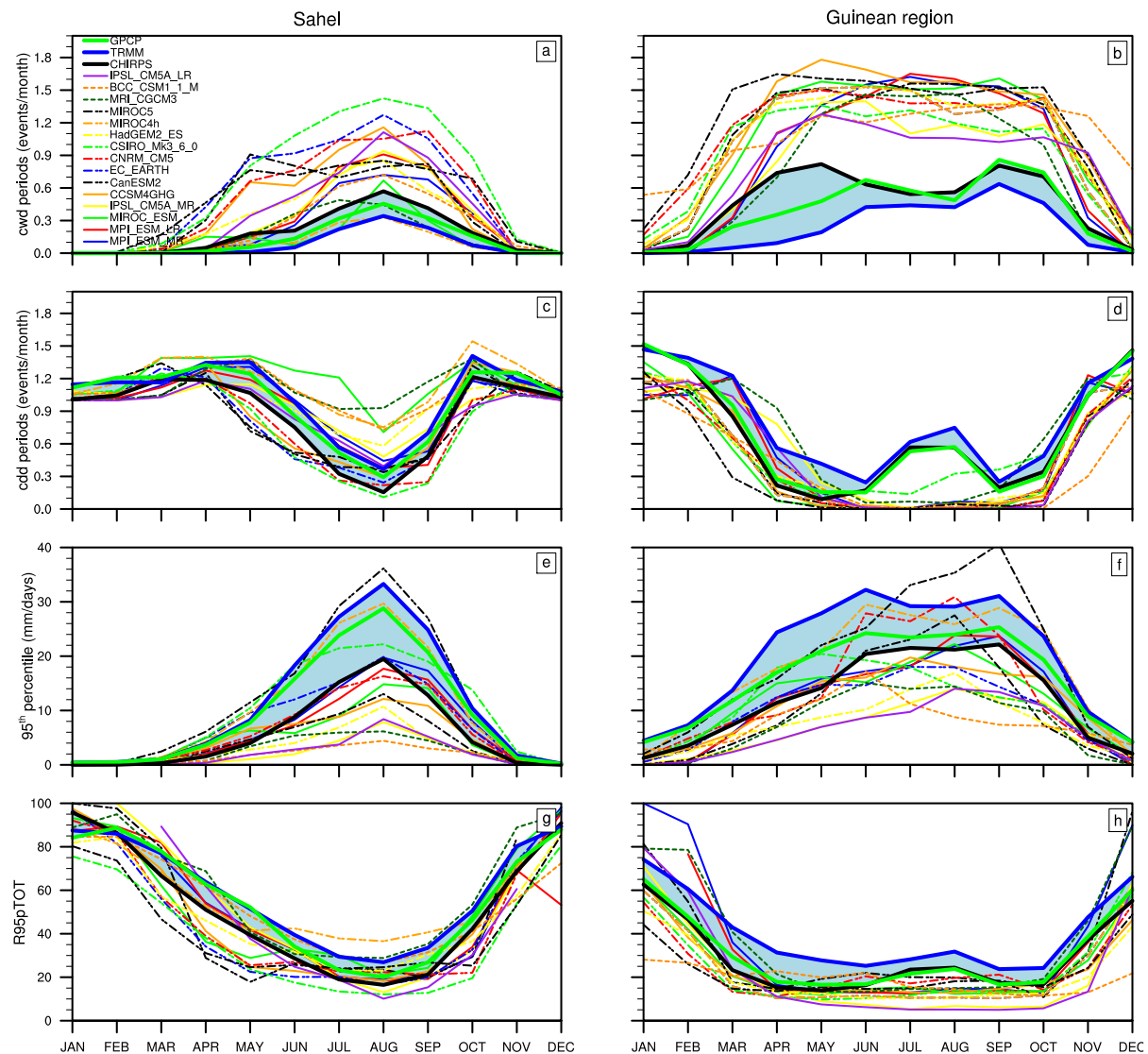
Figure 5. Annual cycle of wet spells (**a,b**), dry spells (**c,d**), 95th percentile (**e,f**) and the fraction of precipitation accounted for by the very wet days (**g,h**) over the Sahel (Left) and the Guinean region (right) from 1985 to 2004 in CHIRPS (black), TRMM (blue), GPCP (green) and 15 models CMIP5 and their ensemble mean (cyan).

Using the Taylor diagrams, these findings have been further quantified (Figure 6). TRMM and GPCP are very strongly correlated (>0.99) with CHIRPS and have standard deviations close to or equal 1 on the annual cycle of CDD over the two regions. As expected from Figure 5a,b, for the CWD, the correlations between either TRMM or GPCP with CHIRPS and the normalized standard deviation are weaker. For CDD, CMIP5 models are weakly correlated with CHIRPS over the Guinean region where the normalized standard deviation is closer to 1; meaning that uncertainties in the annual structure of that index is less important than over the Sahel. On the other hand, for the CWD, distributions along both correlation and standard deviation axes appear highly scattered, pointing to the strong uncertainties qualitatively noted over both regions and on both the temporal evolution and the occurrence of CWD (Figure 6a,b). Regarding now the 95th percentile and R95PTOT indices, their correlations with CHIRPS are higher (>0.90) over both regions, which point to a reasonable simulation

of the temporal evolution of these indices and contrast with their poor skill in terms of standard deviation.
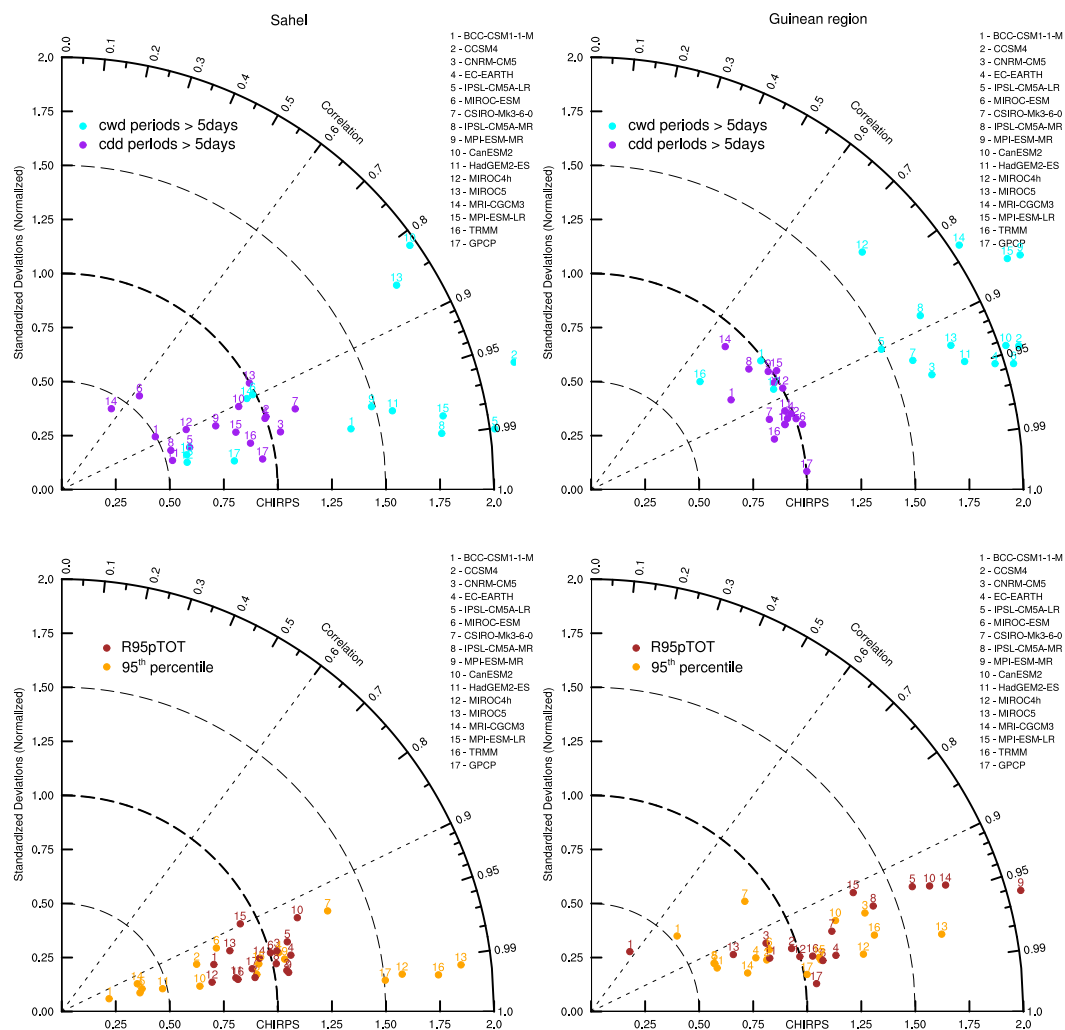
Figure 6. Taylor diagrams of wet spells (cyan), dry spells (purple), 95th percentile (orange) and the fraction of precipitation accounted for by the very wet days (brown) from 1985 to 2004 in the Sahel (left) and the Guinean region (right) on TRMM, GPCP and 15 CMIP5 models compared to CHIRPS.

4. Conclusions and perspectives

In this study, we have analysed how CMIP5 model represents the annual cycle of rainfall characteristics over West Africa, including monthly-mean rainfall as well as other "precipitation variables" including the timing of the monsoon season (onset, cessation) and also the frequency and intensity of daily rainfall, extreme indices such as the percentile 95 and consecutive wet and dry days. We conducted the same analyses for the Sahel and the Guinean region which display distinct annual cycles and precipitation climatology. We considered a total of 15 historical CMIP5 simulations, which have been evaluated with three observational satellite datasets (CHIRPS, TRMM and GPCP) over a 24-year period for CHIRPS and 11-year period for TRMM and GPCP). We further compared the characteristics of the annual cycle of precipitation and precipitation indices with Taylor diagrams and the timing and duration of monsoon rainfall following Liebmann [3]. Over both regions, CHIRPS, TRMM and GPCP are found to agree in their depiction of the annual cycle of the mean precipitation and, to a lesser extend, of the frequency of wet days. However, they provide quite distinct structures of the annual cycles of the intensity of precipitation, especially over the Guinean region. This lack

of agreement in satellite datasets also concerns the 95th percentile or the CWD. This result suggests that further analyses of in-situ precipitation data are needed so as to provide more advanced and valuable observational diagnostics for future model evaluation. Indeed, the magnitude of extreme daily precipitation provided by these satellite datasets can fluctuate by up to 100% during the core monsoon in the Sahel, and distinct structures of the annual cycle of this index are found over the Guinean region with these datasets.

Despite their limitations, these datasets were nevertheless quite useful for evaluating several aspect of the annual cycle of precipitation and precipitation indexes in CMIP5 models, mainly because numerous biases in models were much larger than the spread obtained with satellite datasets.

The performances of the models in simulating the structure of the annual cycle are better over the Sahel than the Guinean region. They are generally able to reproduce the August peak, whereas for the Guinean region, they can be separated in three groups: one group (3 models) which reproduces both the June and September peaks, another (6 models) that reproduces only the first peak and the last group (6 models) only the second peak (usually with a 1-month shift). In terms of amplitude, strong uncertainties in both areas (relatively more pronounced in the Sahel) have been found in the mean precipitation annual cycle, and for most models, these biases generally do not compensate each other when considering precipitation over West Africa, with 66% of the models raining either too much or not enough over both regions. The analysis of intensity and frequency of wet days reveals that over the Guinean area, the uncertainty on total daily precipitation strongly involves the uncertainty associated with the frequency of wet days, whereas in the Sahel, both uncertainties in intensity and frequency are equally important. It must be noted however that models tend to always reproduce a much higher frequency than observed, even when they underestimate the mean precipitation amount (indeed, it rains almost twice more frequently in models than in satellite datasets over the Guinean region).

We found strong uncertainties in the representation of the wet and dry spells (CWD and CDD) over both study areas. Conversely for R95 and R95PTOT, the uncertainties in the annual structure of theses indexes in CMIP5 models appear somewhat weaker in Taylor diagrams, but the magnitude of the R95 in largely underestimated in most models. However, as the contribution of extreme rainfall to the total precipitation is relatively limited (less than 30% during the core monsoon season according to satellite data), the strong uncertainties found on the annual cycle of the intensity and frequency of wet days seem to be associated with errors on either the intensity and frequency of the low and/or moderate daily rainfall events rather than the extreme daily events.

We also found that the annual cycles of precipitation and several precipitation indices are generally very highly correlated (e.g. R95) in both satellite datasets and models. This results points to the importance of a good simulation of the climatological annual cycle of precipitation, and also suggests that its improvement requires advances in the representation of both the intensity and frequency of daily rainfall in models.

This study has highlighted the complexity of the representation the daily rainfall characteristics in climate models and how it translates into large biases at regional scale, which are likely to feedback on the monsoon dynamics [47]. From a smaller scale perspective, we found that, from one precipitation index to another, and according to the area, the uncertainties change dramatically. It is therefore important for each metrics to identify the nature of these uncertainties for impacts studies. Finally, we argue that further studies are necessary in order to understand whether and how these precipitation biases are translated into future projections with climate models over West Africa, in particular shifts in the monsoon season, and changes in mean and extreme precipitation amounts.

5. Patents

This section is not mandatory, but may be added if there are patents resulting from the work reported in this manuscript.

Funding: We acknowledge partial funding from the LMI ECLAIRS2 (Etudes intégrées du climat et de l'océan en Afrique de l'ouest et réponses aux changements climatiques au Sénégal) program.

Acknowledgments: Research leading to this paper has specially done during my Master thesis and I would like to thank the director of LPAO-SF and the Government of Senegal for the financial support. We would also like to thank the NERC/DFID Future Climate For Africa programme under the AMMA-2050 project, grant number NE/M020428/1. Thanks also to Thierry C. Fotso-Nguemo for technical helps.

Conflicts of Interest: The authors declare no conflict of interest.

Abbreviations

The following abbreviations are used in this manuscript:

WAM	West African Monsoon
AEJ	African Easterly Jet
AEWs	African easterly waves
ITCZ	Inter-tropical Convergence Zone
MJO	Madden Julian Oscillation
IPCC	Intergovernmental Panel on Climate Change
RCP	Representative Concentration Pathways
CMIP5	Coupled Model Intercomparison Project phase 5
GHG	Greenhouse Gas
ETCCDI	Expert Team on Climate Change Detection and Indices
SDII	Simple daily intensity index
CDD	Consecutive Dry Days
CWD	Consecutive Wet Days
CHIRPS	Climate Hazards Group Infrared Precipitation with Station

References

1. Fink, A.H.; Engel, T.; Ermert, V.; van der Linden, R.; Schneidewind, M.; Redl, R.; Afiesimama, E.; Thiaw, W.M.; Yorke, C.; Evans, M.; Janicot, S. Mean Climate and Seasonal Cycle. In *Meteorology of Tropical West Africa*; Parker, D.J.; Diop-Kane, M., Eds.; John Wiley & Sons, Ltd; pp. 1–39. doi:10.1002/9781118391297.ch1.
2. Dunning, C.M.; Black, E.C.L.; Allan, R.P. The onset and cessation of seasonal rainfall over Africa: ONSET AND CESSATION OF AFRICAN RAINFALL. *121*, 11,405–11,424. doi:10.1002/2016JD025428.
3. Liebmann, B.; Bladé, I.; Kiladis, G.N.; Carvalho, L.M.V.; B. Senay, G.; Allured, D.; Leroux, S.; Funk, C. Seasonality of African Precipitation from 1996 to 2009. *25*, 4304–4322. doi:10.1175/JCLI-D-11-00157.1.
4. Zipser, E.J.; Cecil, D.J.; Liu, C.; Nesbitt, S.W.; Yorty, D.P. Where are the most intense thunderstorms on earth? *87*, 1057–1072. doi:10.1175/BAMS-87-8-1057.
5. Lebel, T.; Ali, A. Recent trends in the Central and Western Sahel rainfall regime (1990–2007). *375*, 52–64. doi:10.1016/j.jhydrol.2008.11.030.
6. Mathon, V.; Laurent, H.; Lebel, T. Mesoscale Convective System Rainfall in the Sahel. *41*, 1081–1092. doi:10.1175/1520-0450(2002)041<1081:MCSRIT>2.0.CO;2.
7. Frappart, F.; Hiernaux, P.; Guichard, F.; Mougin, E.; Kergoat, L.; Arjounin, M.; Lavenu, F.; Koité, M.; Paturel, J.E.; Lebel, T. Rainfall regime across the Sahel band in the Gourma region, Mali. *375*, 128–142. doi:10.1016/j.jhydrol.2009.03.007.
8. Salack, S.; Muller, B.; Gaye, A.T.; Hourdin, F.; Cisse, N. Multi-scale analyses of dry spells across Niger and Senegal. pp. 3–13. doi:10.1684/sec.2012.0335.
9. Sivakumar, M.V.K. Empirical Analysis of Dry Spells for Agricultural Applications in West Africa. *5*, 532–539. doi:10.1175/1520-0442(1992)005<0532:EAODSF>2.0.CO;2.
10. Mouhamed, L.; Traore, S.B.; Alhassane, A.; Sarr, B. Evolution of some observed climate extremes in the West African Sahel. *1*, 19–25. doi:10.1016/j.wace.2013.07.005.
11. Bechler-Carmaux, N.; Mietton, M.; Lamotte, M. Le risque d'inondation fluviale à Niamey (Niger). Aléa, vulnérabilité et cartographie//River flood risks in Niamey (Niger). Hazards, vulnerability and mapping. *109*, 176–187. doi:10.3406/geo.2000.1888.
12. Zhang, W.; Zhou, T.; Zou, L.; Zhang, L.; Chen, X. Reduced exposure to extreme precipitation from 0.5 °C less warming in global land monsoon regions. *9*. doi:10.1038/s41467-018-05633-3.

13. Sanogo, S.; Fink, A.H.; Omotosho, J.A.; Ba, A.; Redl, R.; Ermert, V. Spatio-temporal characteristics of the recent rainfall recovery in West Africa. *35*, 4589–4605. doi:10.1002/joc.4309.

14. Taylor, C.M.; Belusic, D.; Guichard, F.; Arker, D.J.P.; Vischel, T.; Bock, O.; Harris, P.P.; Janicot, S.; Klein, C.; Panthou, G. Frequency of extreme Sahelian storms tripled since 1982 in satellite observations. *544*, 475–478 +10 p. doi:10.1038/nature22069.

15. Descroix, L.; Guichard, F.; Grippa, M.; Lambert, L.A.; Panthou, G.; Mahé, G.; Gal, L.; Dardel, C.; Quantin, G.; Kergoat, L.; Bouaïta, Y.; Hiernaux, P.; Vischel, T.; Pellarin, T.; Faty, B.; Wilcox, C.; Malam Abdou, M.; Mamadou, I.; Vandervaere, J.P.; Diongue-Niang, A.; Ndiaye, O.; Sané, Y.; Dacosta, H.; Gosset, M.; Cassé, C.; Sultan, B.; Barry, A.; Amogu, O.; Nka Nnomo, B.; Barry, A.; Paturel, J.E. Evolution of Surface Hydrology in the Sahelo-Sudanian Strip: An Updated Review. *10*, 748. doi:10.3390/w10060748.

16. Molua, E.L. Turning up the heat on African agriculture: The impact of climate change on Cameroon's agriculture. *02*, 1–20.

17. New, M.; Hewitson, B.; Stephenson, D.B.; Tsiga, A.; Kruger, A.; Manhique, A.; Gomez, B.; Coelho, C.A.S.; Masisi, D.N.; Kululanga, E.; Mbambalala, E.; Adesina, F.; Saleh, H.; Kanyanga, J.; Adosi, J.; Bulane, L.; Fortunata, L.; Mdoka, M.L.; Lajoie, R. Evidence of trends in daily climate extremes over southern and west Africa. *111*. doi:10.1029/2005JD006289.

18. Lobell, D.B.; Schlenker, W.; Costa-Roberts, J. Climate Trends and Global Crop Production Since 1980. *333*, 616–620. doi:10.1126/science.1204531.

19. Anyamba, A.; Small, J.L.; Britch, S.C.; Tucker, C.J.; Pak, E.W.; Reynolds, C.A.; Crutchfield, J.; Linthicum, K.J. Recent Weather Extremes and Impacts on Agricultural Production and Vector-Borne Disease Outbreak Patterns. *9*, e92538. doi:10.1371/journal.pone.0092538.

20. Sané, O.D.; Gaye, A.T.; Diakhaté, M.; Aziadekey, M. Social Vulnerability Assessment to Flood in Medina Gounass Dakar. *07*, 415–429. doi:10.4236/jgis.2015.74033.

21. Sané, O.D.; Gaye, A.T.; Diakhaté, M.; Aziadekey, M. Critical Factors of Vulnerability That Enable Medina Gounass (Dakar/Senegal) to Adapt against Seasonal Flood Events. *08*, 457. doi:10.4236/jgis.2016.84038.

22. Groupe d'experts intergouvernemental sur l'évolution du climat.; Pachauri, R.K.; Meyer, L.A. *Changements climatiques 2014: rapport de synthèse : contribution des Groupes de travail I, II et III au cinquième Rapport d'évaluation du Groupe d'experts intergouvernemental sur l'évolution du climat*; GIEC. OCLC: 948289514.

23. Biasutti, M.; Sobel, A.H. Delayed Sahel rainfall and global seasonal cycle in a warmer climate. *36*. doi:10.1029/2009GL041303.

24. Allan, R.P.; Soden, B.J. Atmospheric warming and the amplification of precipitation extremes. *321*, 1481–1484. doi:10.1126/science.1160787.

25. Giorgi, F.; Coppola, E.; Solmon, F.; Mariotti, L.; Sylla, M.B.; Bi, X.; Elguindi, N.; Diro, G.T.; Nair, V.; Giuliani, G.; Turuncoglu, U.U.; Cozzini, S.; Güttler, I.; O. Brien, T.A.; Tawfik, A.B.; Shalaby, A.; Zakey, A.S.; Steiner, A.L.; Stordal, F.; Sloan, L.C.; Brankovic, C. RegCM4: model description and preliminary tests over multiple CORDEX domains. *52*, 7–29. doi:10.3354/cr01018.

26. Giorgi, F.; Coppola, E.; Raffaele, F.; Diro, G.T.; Fuentes-Franco, R.; Giuliani, G.; Mamgain, A.; Llopart, M.P.; Mariotti, L.; Torma, C. Changes in extremes and hydroclimatic regimes in the CREMA ensemble projections. *125*, 39–51. doi:10.1007/s10584-014-1117-0.

27. Zwiers, F.W.; Alexander, L.V.; Hegerl, G.C.; Knutson, T.R.; Kossin, J.P.; Naveau, P.; Nicholls, N.; Schär, C.; Seneviratne, S.I.; Zhang, X. Climate Extremes: Challenges in Estimating and Understanding Recent Changes in the Frequency and Intensity of Extreme Climate and Weather Events. In *Climate Science for Serving Society*; Asrar, G.R.; Hurrell, J.W., Eds.; Springer Netherlands; pp. 339–389. doi:10.1007/978-94-007-6692-1_13.

28. Sillmann, J.; Kharin, V.V.; Zhang, X.; Zwiers, F.W.; Bronaugh, D. Climate extremes indices in the CMIP5 multimodel ensemble: Part 1. Model evaluation in the present climate. *118*, 1716–1733. doi:10.1002/jgrd.50203.

29. Panthou, G.; Vischel, T.; Lebel, T. Recent trends in the regime of extreme rainfall in the Central Sahel. *34*, 3998–4006. doi:10.1002/joc.3984.

30. Roehrig, R. Variabilité intrasaisonnière de la mousson africaine : caractérisation et modélisation. p. 411.

31. Monerie, P.A.; Sanchez-Gomez, E.; Boé, J. On the range of future Sahel precipitation projections and the selection of a sub-sample of CMIP5 models for impact studies. *48*, 2751–2770. doi:10.1007/s00382-016-3236-y.

32.   Maidment, R.I.; Grimes, D.; Allan, R.P.; Tarnavsky, E.; Stringer, M.; Hewison, T.; Roebeling, R.; Black, E. The 30 year TAMSAT African Rainfall Climatology And Time series (TARCAT) data set. *119*, 10,619–10,644. doi:10.1002/2014JD021927.

33.   Funk, C.; Peterson, P.; Landsfeld, M.; Pedreros, D.; Verdin, J.; Shukla, S.; Husak, G.; Rowland, J.; Harrison, L.; Hoell, A.; Michaelsen, J. The climate hazards infrared precipitation with stations—a new environmental record for monitoring extremes. *2*, 150066. doi:10.1038/sdata.2015.66.

34.   Huffman, G.J.; Adler, R.F.; Morrissey, M.M.; Bolvin, D.T.; Curtis, S.; Joyce, R.; McGavock, B.; Susskind, J. Global Precipitation at One-Degree Daily Resolution from Multisatellite Observations. *2*, 36–50. doi:10.1175/1525-7541(2001)002<0036:GPAODD>2.0.CO;2.

35.   Huffman, G.J.; Bolvin, D.T.; Nelkin, E.J.; Wolff, D.B.; Adler, R.F.; Gu, G.; Hong, Y.; Bowman, K.P.; Stocker, E.F. The TRMM Multisatellite Precipitation Analysis (TMPA): Quasi-Global, Multiyear, Combined-Sensor Precipitation Estimates at Fine Scales. *8*, 38–55. doi:10.1175/JHM560.1.

36.   Giannini, A.; Saravanan, R.; Chang, P. Oceanic Forcing of Sahel Rainfall on Interannual to Interdecadal Time Scales. *302*, 1027–1030. doi:10.1126/science.1089357.

37.   Janicot, S.; Caniaux, G.; Chauvin, F.; de Coëtlogon, G.; Fontaine, B.; Hall, N.; Kiladis, G.; Lafore, J.P.; Lavaysse, C.; Lavender, S.L.; Leroux, S.; Marteau, R.; Mounier, F.; Philippon, N.; Roehrig, R.; Sultan, B.; Taylor, C.M. Intraseasonal variability of the West African monsoon. *12*, 58–66. doi:10.1002/asl.280.

38.   Sylla, M.B.; Giorgi, F.; Pal, J.S.; Gibba, P.; Kebe, I.; Nikiema, M. Projected Changes in the Annual Cycle of High-Intensity Precipitation Events over West Africa for the Late Twenty-First Century. *28*, 6475–6488. doi:10.1175/JCLI-D-14-00854.1.

39.   Zhang, X.; Alexander, L.; Hegerl, G.C.; Jones, P.; Tank, A.K.; Peterson, T.C.; Trewin, B.; Zwiers, F.W. Indices for monitoring changes in extremes based on daily temperature and precipitation data. *2*, 851–870. doi:10.1002/wcc.147.

40.   Adejuwon, J.O.; Odekunle, T.O. Variability and the Severity of the "Little Dry Season" in Southwestern Nigeria. *19*, 483–493. doi:10.1175/JCLI3642.1.

41.   Diedhiou, A.; Janicot, S.; Viltard, A.; de Felice, P.; Laurent, H. Easterly wave regimes and associated convection over West Africa and tropical Atlantic: results from the NCEP/NCAR and ECMWF reanalyses. *15*, 795–822. doi:10.1007/s003820050316.

42.   Mohr, K.I.; Thorncroft, C.D. Intense convective systems in West Africa and their relationship to the African easterly jet. *132*, 163–176. doi:10.1256/qj.05.55.

43.   Guichard, F.; Petch, J.; Redelsperger, J.L.; Bechtold, P.; Chaboureau, J.P.; Cheinet, S.; Grabowski, W.; Grenier, H.; Jones, C.; Köhler, M.; Piriou, J.M.; Tailleux, R.; Tomasini, M. Modelling the diurnal cycle of deep precipitating convection over land with cloud-resolving models and single-column models. *130*, 3139–3172. doi:10.1256/qj.03.145.

44.   Roehrig, R.; Bouniol, D.; Guichard, F.; Hourdin, F.; Redelsperger, J.L. The Present and Future of the West African Monsoon: A Process-Oriented Assessment of CMIP5 Simulations along the AMMA Transect. *26*. doi:10.1175/JCLI-D-12-00505.1.

45.   Diallo, F.B.; Hourdin, F.; Rio, C.; Traore, A.K.; Mellul, L.; Guichard, F.; Kergoat, L. The Surface Energy Budget Computed at the Grid-Scale of a Climate Model Challenged by Station Data in West Africa. *9*, 2710–2738. doi:10.1002/2017MS001081.

46.   Seth, A.; Rauscher, S.A.; Biasutti, M.; Giannini, A.; Camargo, S.J.; Rojas, M. CMIP5 Projected Changes in the Annual Cycle of Precipitation in Monsoon Regions. *26*, 7328–7351. doi:10.1175/JCLI-D-12-00726.1.

47.   Biasutti, M.; Voigt, A.; Boos, W.R.; Braconnot, P.; Hargreaves, J.C.; Harrison, S.P.; Kang, S.M.; Mapes, B.E.; Scheff, J.; Schumacher, C.; Sobel, A.H.; Xie, S.P. Global energetics and local physics as drivers of past, present and future monsoons. *11*, 392–400. doi:10.1038/s41561-018-0137-1.

Sample Availability: Samples of the compounds ...... are available from the authors.